



Contents lists available at ScienceDirect

Construction and Building Materials

journal homepage: www.elsevier.com/locate/conbuildmat

Synergy between crystalline admixtures and nano-constituents in enhancing autogenous healing capacity of cementitious composites under cracking and healing cycles in aggressive waters



Estefania Cuenca*, Alessandro Mezzena, Liberato Ferrara

Department of Civil and Environmental Engineering, Politecnico di Milano, Piazza Leonardo da Vinci 32, 20133 Milano, Italy

HIGHLIGHTS

- The healing capacity in aggressive scenarios has been studied in HPCFRCC specimens.
- Three types of nano-constituents were incorporated to HPCFRCC.
- Alumina nanofibers and cellulose (nanocrystals and nanofibers) were employed.
- Mechanical and durability performance have been analyzed.

ARTICLE INFO

Article history:

Received 27 April 2020

Received in revised form 7 October 2020

Accepted 20 October 2020

Available online 9 November 2020

ABSTRACT

More than one century after its massive introduction in the building industry, concrete is still the most popular building material. Nevertheless, several critical infrastructures show severe signs of distress. This fact fostered, in recent years, the need of rethinking the design process of concrete structures, in view of reducing maintenance costs and extending their service life. This work has been performed in the framework of the H2020 project ReSHEALience (GA760824). The main idea behind the project is that the long-term behaviour of structures under extremely aggressive exposure conditions can highly benefit from the use of high performance materials, in the framework of durability-based design approaches. The project will tailor the composition of Ultra High Durability Concrete (UHDC), by upgrading the High-Performance Cementitious Composite/High-Performance Fibre Reinforced Cementitious Composite (HPCC/HPFRCC) concept through the incorporation of tailored nanoscale constituents focusing, among the others, on stimulating the autogenous self-healing capacity. This work shows the effectiveness of the aforementioned concept achieved through the incorporation in a reference HPFRCC of three types of nano-constituents: alumina nanofibers (0.25% by weight of cement), cellulose nanocrystals (0.15% by weight of cement) and cellulose nano-fibrils (0.15% by weight of cement). The influence of the nano-constituents has been analysed in terms of mechanical properties, such as flexural and compressive strength and on shrinkage and durability properties, analysed by means of sorptivity tests on uncracked, cracked and self-healed specimens with reference to selected aggressive exposure scenarios representative of intended engineering applications of the investigated materials.

© 2020 The Author(s). Published by Elsevier Ltd. This is an open access article under the CC BY-NC-ND license (<http://creativecommons.org/licenses/by-nc-nd/4.0/>).

1. Introduction

The signature tensile behaviour of High-Performance Fibre Reinforced Cementitious Composites (HPFRCCs) is characterized by stable multiple cracking resulting through related stress redistribution into strain-hardening response [1] which is particularly interesting for the structural service life. This can be obtained

thanks to a tailored material composition, designed according to a balance between crack-tip toughness and fibre pull-out energy, which, as widespread demonstrated by the abundant literature on the topic [2], is characterized, among the others, by (very) high content of cement and binder and low water-to-binder ratios, besides volume fractions of fibres usually in some percentage units range. As a matter of fact, this category of materials is quite often “labelled” and promoted primarily through high compressive strength values, with “customary” requests ranging from 120 to 150 MPa and even more, depending on the standards and jurisdiction [3]. Quantification of tensile mechanical performance in terms

* Corresponding author.

E-mail addresses: estefania.cuenca@polimi.it (E. Cuenca), alessandro.mezzena@polimi.it (A. Mezzena), liberato.ferrara@polimi.it (L. Ferrara).

of strength and ultimate tensile deformation capacity has been so far provided in much more scattered terms and only recently a classification has been proposed by related French standards [4] only based on ultimate to first average and characteristic strength ratios. The use of aggregates with a very small maximum aggregate diameter (2–10 mm) favour a high compactness and a very low porosity of the matrix which confer a very high durability to concrete in un-cracked state. As a matter of fact, the same material composition which is responsible for the high matrix compacted and for the tensile strain-hardening characterized by the stable formation of multiple tiny cracks is also highly conducive to autogenous healing, primarily due to the delayed and continuous hydration and hydraulic/pozzolanic reactions of the high amounts of cement and binders, not reacted with the initially low available water quantity in the mix [5].

Autogenous self-healing capacity of high performance fibre reinforced cementitious composites has been extensively studied by several research groups worldwide [6–10], assessing the role of the initial crack width, aggressive exposure conditions, age and repeatability of cracking as well as of sustained through-crack stress not only of the capacity of the material to seal the cracks and recovery its “imperviousness” against different transport phenomena and on the kinetics of the crack-sealing processes, but also on the level of retention of the tensile load-bearing and ultimate deformation capacity [11–17]. This last information is, as a matter of fact, of the utmost importance to incorporate the effects and benefits of self-healing into a durability-based conceptual design approach of structures made of/retrofitted with the category of materials investigated in this paper.

The role of different types of fibres has also been investigated, highlighting, e.g., that natural fibres and super-absorbent polymers can develop and effective synergy with other types of fibre reinforcement, being able to absorb, store and transport water (the crack-healing agent) to the cracked site, being also instrumental in improving the repeatability, persistence and robustness of the healing phenomena [18–24].

Other researchers have also investigated the effects of healing stimulators, such as crystalline admixtures, when added, at dosages suitably adapted to the high content of cements of HPFRCCs, [25–26]. They found, for example, that the somewhat expansive characteristics of the stimulated healing reactions occurring at multiple cracking sites may also result into a sort of “smeared” chemical pre-stressing of the homogeneously dispersed fibre reinforcement, with systematic enhancement along the healing time of the mechanical performance of the material.

As a matter of fact, the benefits of materials combining superior mechanical performance with enhanced long-term durability, further empowered by self-healing functionalities, can find their most relevant and highly rewarding applications in structures subjected to extremely aggressive environments. The research community has only recently started to investigate such scenarios and has mainly focused on chloride attack [16,27]. In this framework, the ReSHEALience project consortium, funded by the European Commission through the Horizon2020 Research and Innovation Programme, has proposed a holistic material and structural concept and design approach for structures made of/retrofitted with Ultra High Durability Concrete in aggressive structural service scenarios which encompass, besides chloride attack, also chemical aggression, e.g. by sulphates and acids [28]. While structures and infrastructures in marine environments including offshore are a clear example representing of the former scenario, urban sewage networks as well as facilities serving geothermal site plants can be called as representative of the latter, the social and economic values of all of the cited examples being self-evident.

In all the aforementioned cases, besides the severity of the environmental attack, demands for high mechanical performance also

hold, because of, e.g., cyclic wave/water actions and surface wear/erosion also due to the transport of solid particles by the fluids the structure interacts with. The solution implemented by the ReSHEALience consortium has worked, in order to upgrade the current HPFRCC concept to that of a Ultra High Durability Concrete (UHDC), to exploit the synergy between self-healing stimulation via crystalline admixtures and nano-scale functionalization, in detail put into effect through alumina nano-fibres and cellulose nano-fibrils and nano-crystals. The key ideas is that, besides the usual and well known matrix densification and hydration stimulation roles, the employed nanoparticles can really play an active role as reinforcement at the very molecular level of the material and acting in synergy with healing stimulators in governing and modifying the degradation mechanisms and phenomena since their very onset and initiation. This with the strategic conceptual vision of transforming the material from passive provider of protection against ingress of aggressive species into an active player able to respond to degradation processes as a function of the performance demands of the engineering application.

This paper contains the results of a study aimed at preliminarily assessing the effects of the aforementioned synergy on the mechanical and healing performance in high performance fibre reinforced mixes all containing a crystalline healing stimulator and functionalized with the addition of either alumina nano-fibres or nano-cellulose fibrils and crystals when exposed, since their early curing, to conditions represented by water from geothermal drilling.

The use of alumina nanofibers is quite a novelty in the field of concrete and cement-based materials technology. In most of the few related studies [29–32], their beneficial effect, when added at less than 1% by weight of cement, have been shown on the compressive strength and other specific mechanical properties of a variety of cementitious materials. These range from HPFRCCs, in which case also a good interaction with the employed polyethylene or poly-vinyl-alcohol fibre reinforcement was measured through enhanced flexural deformation capacity, to oil well slurries, for which, besides moderate improvement also in splitting tensile strength, stability of the rheological performance upon their incorporation was also studied. Higher dosages, up to several percentage units (5–7%) by weight of cement, were used by some researchers [33–34] to improve freeze and thaw resistance or high temperature behaviour. The detected improvements common to all the surveyed investigations have been explained on the one hand considering that alumina nanofibers, which contain free hydroxyl groups on their surface, act as nucleation site for hydration of cement particles. On the other hand, it has been also highlighted that, because of their size, aluminium oxide nanofibers can act as reinforcement of the layered CSH structure thus reducing the shrinkage deformation and providing a nano-structural toughening effect. In all cases, the need has been highlighted to provide a suitably dispersed suspension to be easily handled with the mixing procedure of cement based materials as well as to likewise suitably take into account the compatibility with the employed superplasticizer type.

On the other hand, the use of nano-cellulose in cementitious composites is fairly better documented, as also witnessed by recently published state of the art review papers on the topic [35]. Insight has been gained into interaction mechanisms which cement particles by nano-cellulose ones which, acting as nuclei for hydration and distributed water reservoirs, affect the hydration process, accelerating it and stimulating the production of more portlandite and calcium silicate gel. This also affects the rheological properties, generally resulting into a stiffening of the composites, the volume stability, with consequent reduction of autogenous shrinkage, and the mechanical properties, with measured improvements in compression and flexural strength

[36–40]. Also in the case of nano-cellulose products, as common to alumina nanofibers and all other nanoparticles, the importance has been highlighted of a proper dispersion, customarily through ultrasonication and also an appropriate interaction with the superplasticizer, to obtain a homogenous composite material where the benefits of nano-constituents could be effectively exploited.

As already stated above, the aim of the present investigation, conceived and performed in the framework of the ReSHEALience project, is to assess the influence of alumina nano-fibres and nano-cellulose fibrils and crystals, on the evolution of the mechanical properties (compressive and flexural strength, flexural toughness) of high performance fibre reinforced cementitious composites exposed since their very early ages (one day after casting) to aggressive waters such as those from drilling operations in geothermal power plants (containing both chlorides and sulphates). Moreover, the synergy has been assessed of the aforementioned nano-constituents with crystalline admixtures in stimulating the autogenous healing of the same composites, when exposed to the same scenario, and the related recovery of the imperviousness, as measured by means of through-crack capillary water absorption.

Such a synergy, as stated above, is meant to provide experimental evidence to the Ultra High Durability Concrete material concept on which the ReSHEALience project is working, and which aims, rightly through “nano-engineering” of the material composition, to enforce a conceptual paradigm shift into the design approach to durability of high performance cement-based materials and related structural applications: the material has not to be regarded any more as a mere provider of passive protection against the ingress of aggressive species into the structural element but is able to actively self-govern its intrinsic structure evolution under the anticipated aggressive structural service scenario, being thus able to provide an evolution of its “in-structure” performance coherent with the demand all along the structure service life.

2. Materials

The reference mix for the study reported in this paper is a High Performance Fibre Reinforced Cementitious Composite, whose composition is detailed in Table 1 under the XA-CA-REF acronym. Starting from a typical HPRCC mix already extensively studied by the authors [6,7,41,42], appropriately conceived also to be employed in acid attack environment (high replacement of cement type I with slag), it has been further added with Penetron Admix[®] Crystalline Admixture (CA) as a stimulator of the autogenous self-healing capacity. Table 2 reports the properties of the employed cement and slag.

Table 1

Mix-composition of investigated HPRCCs/UHDCs (in kg/m³ if not otherwise specified).

Constituents	XA-CA REF	XA-CA CEMIII	XA-CA + ANF	XA-CA +CNC	XA-CA + CNF
CEM I 52,5 R	600	–	600	600	600
CEM III	–	600	–	–	–
Slag	500	500	500	500	500
Water	200	200	200	200	200
Steel fibers [®]	120	120	120	120	120
Azichem Readymesh 200	–	–	–	–	–
Sand 0–2 mm	982	982	982	982	982
Superplasticizer	33	33	33	33	33
Glenium ACE 300 [®]	–	–	–	–	–
Crystalline Admixture	4.8	4.8	4.8	4.8	4.8
Alumina nanofibers*	–	–	0.25	–	–
Cellulose nanocrystals*	–	–	–	0.15	–
Cellulose nanofibrils*	–	–	–	–	0.15

* % by weight of cement.

Table 2

Composition of the employed cement and slag (contents by % weight).

Chemical constituent	CEM I	Slag
SiO ₂	38.9	39.2
CaO	59.7	38.9
Al ₂ O ₃	4.9	10.2
MgO	3.3	6.4
SO ₃	3.4	1.3
Mn ₂ O ₃ /MnO	0.1	0.3
Fe ₂ O ₃	3.5	0.4
TiO ₂	0.2	0.6
K ₂ O	0.2	0.8
Na ₂ O	0.4	0.3
other	0.4	0.3
Loss on ignition at 1000 °C	2.5	1.2

As well known, crystalline admixtures are proprietary mixtures of active chemicals in a carrier of cement and sand, which are able to react with either cement particles or cement hydration products, or both, and produce modified calcium silicate hydrate products. Crystalline admixtures are characterized by particles of irregular shape ranging from 1 to 20 μm with presence of calcium, oxygen, silicon, magnesium, aluminium and potassium [43]. These, besides refining the pore structure and hence enhancing the durability of the admixture cementitious composite in the un-cracked state, are also able, where produced at a cracked site and precipitating onto cracked surfaces, to promote a faster sealing of the same cracks. Moreover, the employed crystalline admixture, whose morphological and chemical characteristics have been already described by [43–46] has been already employed by the authors as an autogenous healing stimulator in conventional plain and fibre-reinforced concrete [47] and in HPRCCs [25]. The authors highlighted an interesting synergy with the dispersed fibre reinforcement resulting into enhanced capacity of retaining, if not improving along the healing time, the mechanical performance of the composites thanks to a sort of chemical fibre pre-stressing action, which is likely to be activated exactly at the cracked-healing sites by the healing products. These, in fact, besides sealing the cracks, and hence reconstituting the through crack continuity of the cementitious matrix, also act at the fibre–matrix interface level, enhancing the fibre–matrix bond through deposition of healing products along the same interface. In view of these previous findings, the CA above has been employed as a reference constituent throughout this investigation in synergic combination with selected nanoparticles. Its dosage has been set at 0.8% by weight of cement, considering the high cement content which the composition of HPRCCs normally feature, whereas the recommended dosage in the case of conventional concrete ranges from 1.0 to 1.5% by weight of cement.

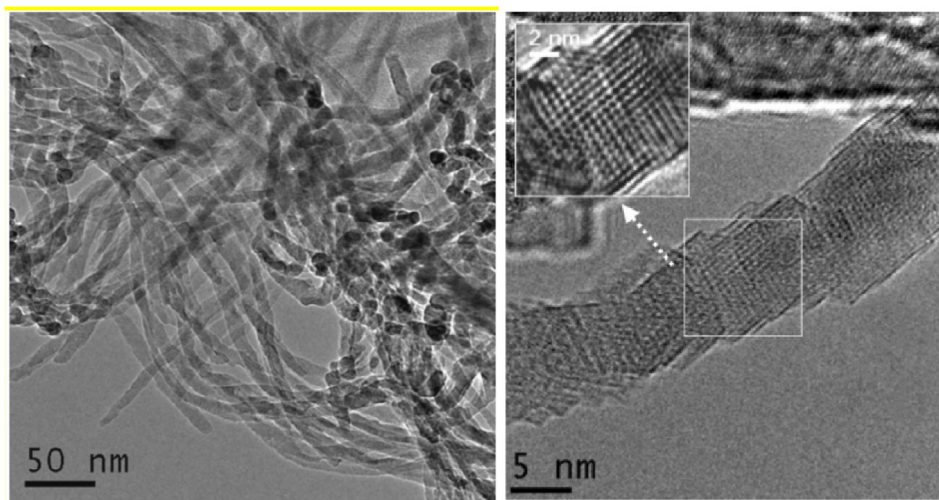


Fig. 1. Microscope images of employed alumina NAFEN® nanofibers (courtesy of dr. Aleksej Tretjakov and Dennis Lizunov NAFEN®).

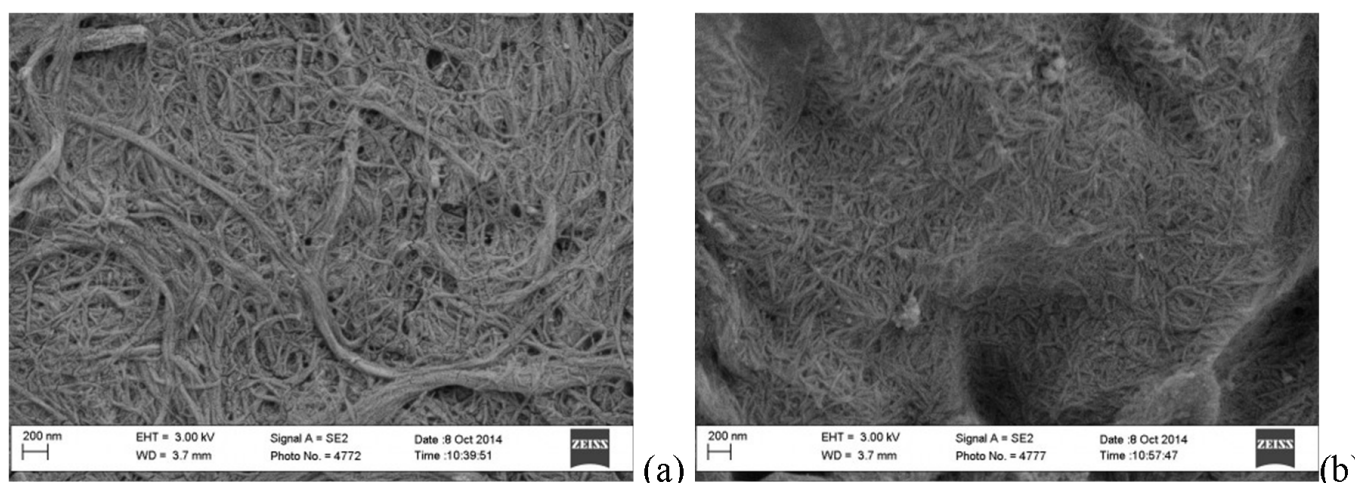


Fig. 2. Microscope images of employed cellulose nanofibrils (a) and nanocrystals (b).

Aluminium oxide nanofibers employed in this investigation (NAFEN®) have a length ranging between 100 and 900 nm and a diameter of 4–11 nm, with a surface area of 155 m²/g (Fig. 1). They have been provided in a suspension at 10% nanofiber concentration, developed through a tailored ultrasonic dispersion and disintegration multi-stage treatment process, and stabilized also through the use of a poly-carboxylate sodium salt admixture. As from mix optimization studies performed in the framework of the project activities, alumina nanofibers have been added to the mix at a dosage equal to 0.25% by weight of cement (referred to the effective fibre content), as specified in Table 1 under the XA-CA-ANF acronym.

Nano-cellulose has been employed in this study in two different forms of fibrils and crystals. The employed nano-fibrils have dimensions ranging from 5 to 20 nm in diameter and from 50 to >2000 nm in length, whereas the nanocrystals, with an average diameter of 5 nm, have lengths from 50 to 500 nm (Fig. 2a-b). An extensive characterization of the microstructure of the employed nano-cellulose products has been performed in [48] highlighting high crystallinity index (>97%).

Also in this case, based on mix composition and mixing protocol optimization studies, both cellulose nanofibrils and nanocrystals have been added into the cementitious composite mix at a dosage

Table 3
Grain size distribution of employed sand.

Sieve diameter (mm)	% passing	Cumulative passing (%)
0	0	0
0.2	14.6	14.6
0.35	9.7	24.3
0.45	9.7	34
0.6	9.7	43.7
1.0	19.7	63.4
1.5	18.3	81.7
2.0	18.3	100

equal to 0.15% by weight of cement, always referred to the effective fibre content (see in Table 1 under the labels XA-CA-CNF and XA-CA-CNC). It is also worth here remarking that both nanocellulose products (AVAP®) were supplied in the form of an aqueous suspension at 10% solid concentration, specifically design for the purposes of the ReSHEALence project activities and applications. A predilution at 6% concentration was recommendedly performed before adding them into the mix.

Besides the mixes described above, a further mix was produced replacing CEM type I, employed in all mixes, with CEM type III

Table 4
Composition of the geothermal water employed for specimen curing and healing.

Constituent	Al	Ca	Fe	K	Mg	Na	S	Si	SO ₄ ²⁻	Cl
ppm	0.2	4	0.13	19.8	0.3	1243.2	1523.4	0.3	2678	441

Table 5
Experimental program.

Test	Number of specimens / mix	Test details
Compressive and flexural tests according to EN 1015	9	Compressive and flexural strength specimens cured in moist room (20 °C, 95% RH) and tested at: 28 days (3 specimens/mix), 56 days (3 specimens/mix), 84 days (3 specimens/mix).
	9	Compressive and flexural strength specimens immersed in geothermal water and tested at: 28 days (3 specimens/mix), 56 days (3 specimens/mix), 84 days (3 specimens/mix).
Total (drying) and autogenous shrinkage tests	3	Total (drying) shrinkage tests on specimens cured in climate room (20 °C, 50% RH).
Sorptivity tests and visual crack observations	3	Autogenous shrinkage tests on specimens cured in climate room (20 °C, 50% RH).
	6	Subjected to sorptivity tests according to the following scheme: Specimens were pre-cracked and subjected to sorptivity tests and visual crack observations with optical microscope. Subjected to wet/dry cycles (3 specimens/mix) and immersed in geothermal water (3 specimens/mix). After 1 month they were subjected to sorptivity tests and visual crack observations. Then they were re-cracked and subjected to sorptivity tests and visual crack observations. Same procedure was repeated after 3 and 6 months.
	6	Subjected to sorptivity tests according to the following scheme: Specimens were pre-cracked and subjected to sorptivity tests and visual crack observations with optical microscope. Subjected to wet/dry cycles (3 specimens/mix) and immersed in geothermal water (3 specimens/mix). After 1 month they were subjected to sorptivity tests and visual crack observations. Same procedure was repeated after 3 and 6 months.
Mercury porosimetry test (MIP)	1	Specimen cured in moist room (20 °C, 95% RH) was subjected to MIP test.
Thermogravimetric analysis (TGA)	1	Specimen immersed in geothermal water was subjected to MIP test.
	1	Specimen cured in climate room (20 °C, 50% RH) was subjected to TGA.
	1	Specimen immersed in geothermal water was subjected to TGA.

(whose characteristics and properties, as from X-ray fluorescence, are reported in Table 2). This, besides the needs dictated by the acid attack scenario, was also meant to check the long term mechanical and durability performance of a HPFRCC with low clinker and high slag content. As a matter of fact, the performance of the mix may on the one hand be favoured by the delayed and

latent hydraulic activity of the slag, which, on the other hand, may be poorly activated by the low content of clinker and hence by the low and slow production of calcium hydroxide.

As can be also seen in Table 1, all mixes contained sand with 2 mm maximum aggregate size, with grain size distribution reported in Table 3, and were reinforced with 120 kg/m³

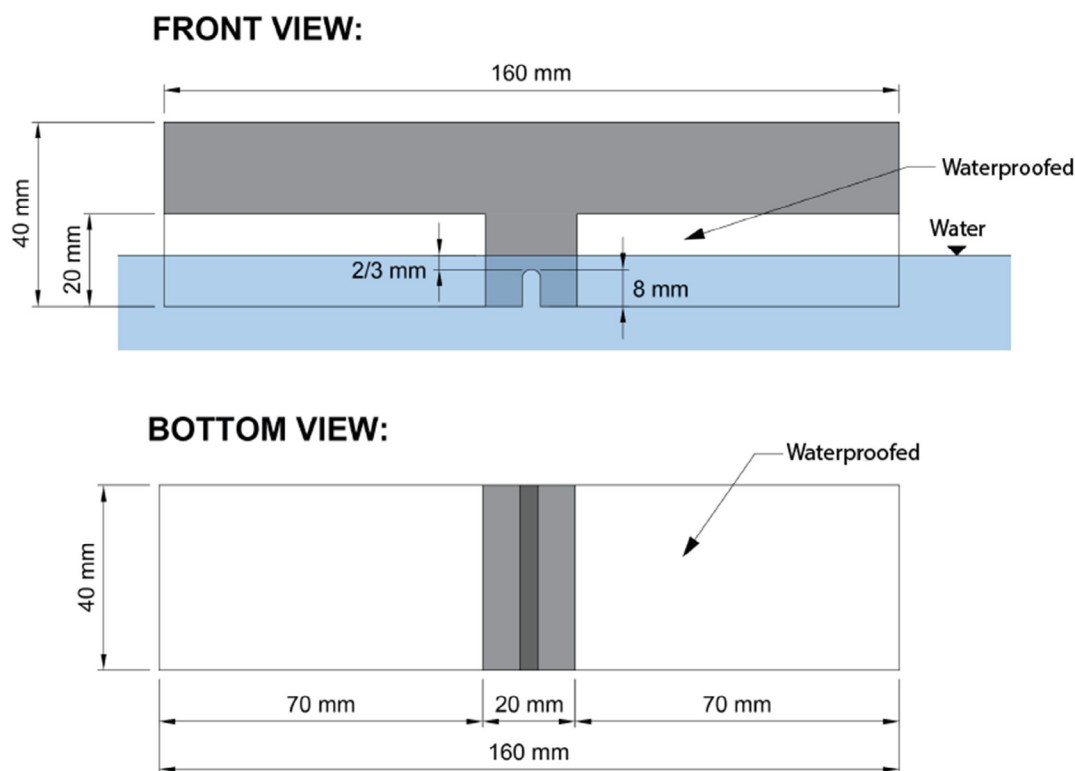


Fig. 3. Schematic of the sorptivity test set-up.





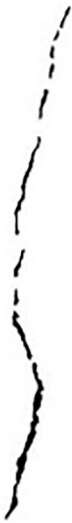
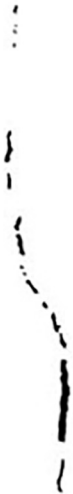
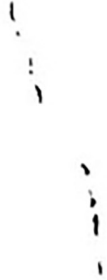
Time 0 (pre-cracking)	1 month (healed)	3 months (healed)	6 months (healed)
			
			$A_{\text{crack, 6 months healing}} = 0$ $ICS = 1$
$A_{\text{crack, pre-cracking}}$ $ICS = 0$	$A_{\text{crack, 1 month healing}}$ $0 < ICS < 1$	$A_{\text{crack, 3 months healing}}$ $0 < ICS < 1$	

Fig. 4. Graphical explanation of the procedure for crack sealing evaluation and calculation of Index of Crack Sealing ICS.

($V_f = 1.5\%$) straight steel fibres, 20 mm long and with a 0.22 mm diameter (aspect ratio ≈ 90), such a dosage having been chosen, also on the basis of previous optimization studies, to cope with the strain hardening tensile deformability requirements dictated by the intended application [49].

3. Experimental program

With each and all the mixes described in Table 1, $40 \times 40 \times 160$ mm beams were cast which were employed for the experimental program detailed hereafter:

- 3-point flexural tests performed in displacement control at a $0.5 \mu\text{m}/\text{sec}$ speed; an 8 mm deep notch was cut at mid-span of the specimens to localize the fracture and ease the measurement of a Crack Mouth Opening Displacement (CMOD). Flexural tests were performed at 28, 56 and 84 days on specimens which were cured either in a climate room at 20°C and 95%RH or immersed in geothermal water since one day after casting. The water was directly obtained from cooling water basing in the geothermal power plant operated by the ReSHEALience project partner Enel Green Power (EGP) in Chiusdino, Italy. Its composition is shown in Table 4 and highlights high concentration

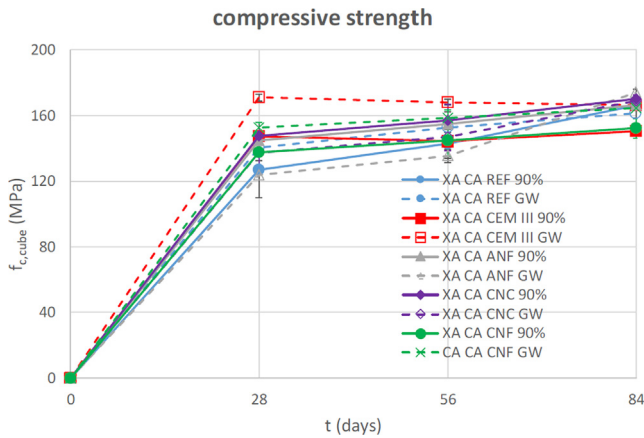


Fig. 5. Compressive strength vs. time for investigated cementitious composites in different curing environments.

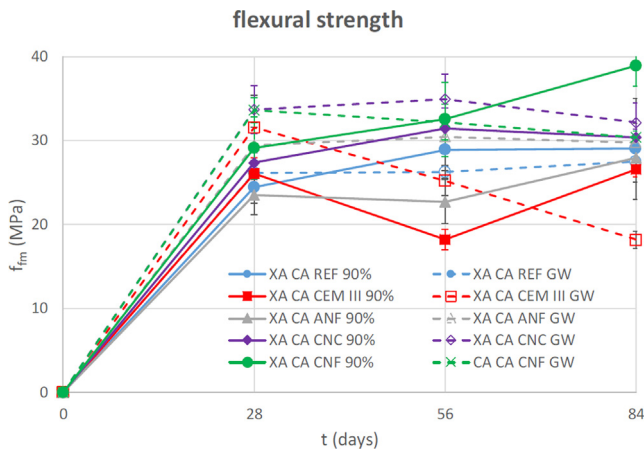


Fig. 6. Flexural strength vs. time for investigated cementitious composites in different curing environments.

of both sulphur and sulphate ions besides sodium and chloride ions, aggressive for both the cementitious matrix and the steel fibre reinforcement respectively. For each curing condition and each testing age, three nominally identical specimens were tested.

- Compressive strength tests were performed according to the Standard EN 1015-11-1999. To this purpose, the specimen halves obtained by breaking the specimens by flexure ($40 \times 40 \times 80$ mm samples) were used and the force was

applied by two plates 40×40 mm long and 10 mm thick as indicated in the Standard EN 1015-11-1999. Testing ages and curing conditions were the same as for flexural tests. Consistently, six specimens were tested in compression for each curing condition and testing age.

- Total (drying) and autogenous shrinkage tests: three specimens for each mix and each shrinkage type measurement were employed; specimens were stored in a climate room at 20 °C and 50% RH.
- Self-healing tests via sorptivity measurements after immersion and/or wet-and-dry cycles in the same geothermal water described in Table 4. In total twelve specimens per each mixed were used for this part of the investigation, six being kept completely immersed in the water and six subjected to wet and dry cycles. Sorptivity tests were first performed, according to the methodology based on EN 13057 which will be hereafter described in detail. Then all specimens were pre-cracked at an age of at least 56 days up to a nominal CMOD of 150 μ m. The hydration should also proceed after the 56 days due to the formation of the crack. In fact, the crack is a new path that appear in the concrete matrix allowing further hydration reactions of cement particles and hence promoting healing reactions [27]. After the pre-cracking all cracks were mapped with a digital microscope and sorptivity tests were performed once again to mark the difference in water capillary absorption immediately before and after the cracking. The healing procedure then started, via immersion in geothermal water, permanent or alternating three days in water and four days in a climate room at 50% RH and 20 °C. After one month the specimens were taken out of the healing environment and cracks were mapped once again via the digital microscope image acquisition. Sorptivity tests were performed once again as well. Before performing the sorptivity test the specimens were dried in an oven at 40 °C until a constant weight was achieved and then kept in the climate room (20 °C, 50% RH) for 24 h. At the end of the first scheduled deadline, half of the specimens for each mix continued to do the healing procedure as such (either immersed or subjected to wet and dry cycles) whereas the other half, before going back to the healing environment were re-cracked up to a further nominal crack opening of 150 μ m. The same procedure was repeated after three and six months from first pre-cracking.

A synopsis of the experimental program as a whole is provided in Table 5.

For the sorptivity tests, the specimens were put on two supports into a layer of water so to have a 5 mm water height above the notch tip (Fig. 3). In order to limit the water uptake only through the crack, a layer of silicone was applied all along the bot-

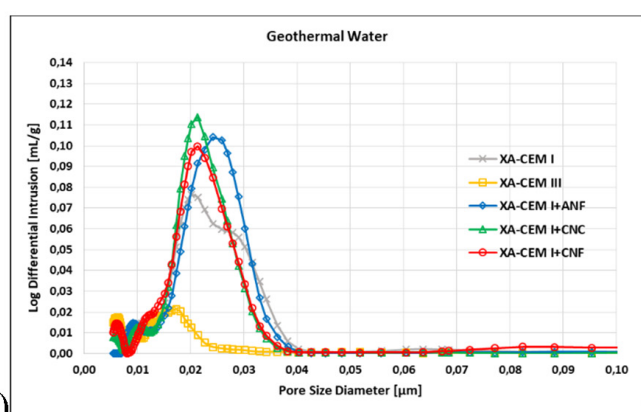
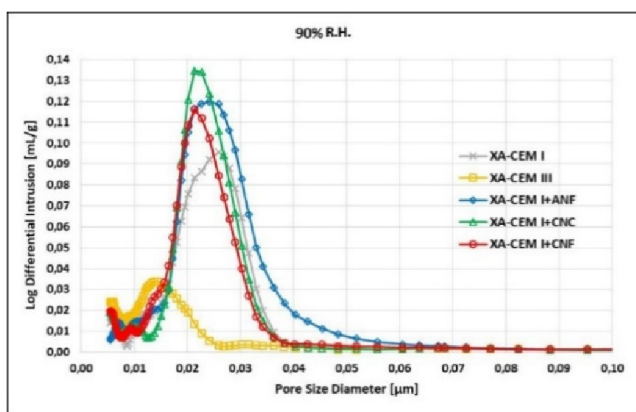


Fig. 7. MIP test results for investigated cementitious composites cured in 20 °C-90%RH climate room (a) and in geothermal water (b).

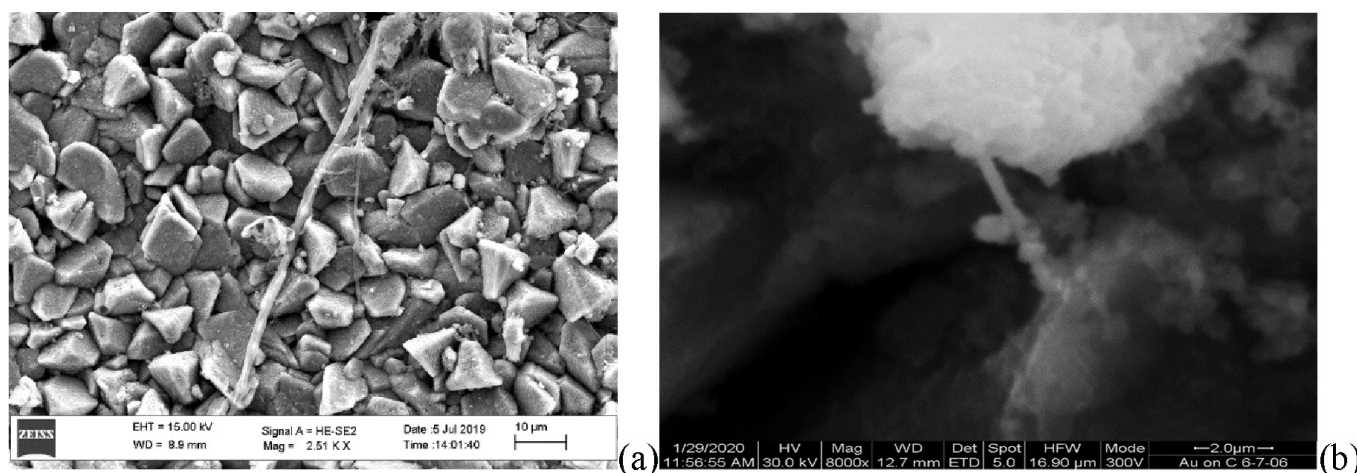


Fig. 8. SEM images of microstructure of investigated cementitious composites reinforced with alumina nanofibers (a – also courtesy of dr. Aleksej Tretjakov and Dennis Lizunov NAFEN[®] and prof. Olga Volobujeva – Tallin University of Technology) and nanocellulose fibrils (b) (also courtesy of dr. Evangelia Entze and Stamatina Sideri, API Europe[®]).

tom half of the specimen outer surface so to leave free only a 20 mm wide zone across the crack and the notch. The silicone layer was renovated at each time. As remarked above, specimens were dried in the oven at 40 °C and then kept in the dry room for 24 h at each testing deadline before performing the sorptivity measurements. For the latter, water uptake was measured by weighing the specimens 15 min, 30 min, 1 h and then at 1 h intervals after putting them in the water and up to 8 h.

Evaluation of the healing was performed via both visual assessment of crack closure and recovery of water permeability as assessed in the sorptivity tests performed as above.

For the former, by means of suitable image processing of the crack images acquired after pre-cracking and after scheduled healing/re-cracking steps, the total area of the crack was calculated [46] and crack sealing was quantified by means of the following: Crack Sealing Index

$$ICS = 1 - \frac{A_{\text{crack, after healing}}}{A_{\text{crack, after 1st pre-cracking}}}$$

according to the procedure graphically explained in Fig. 4.

For the latter, by plotting the water uptake measurements vs. the square root of the time, the sorptivity coefficients was first obtained as the slope of the thus plotted water uptake curve in the stable regime. Then, by comparing the values of the sorptivity coefficient calculated as above immediately after pre-cracking and after scheduled healing times, an Index of Sorptivity Healing, also meant as an Index of material performance healing, was calculated as follows:

Sorptivity Healing Index

$$ISH = 1 - \frac{\text{Sorptivity coefficient}_{\text{after healing}}}{\text{Sorptivity coefficient}_{\text{after 1st pre-cracking}}}$$

Macroscopic material performance healing observations were complemented with the following microstructural investigation tests:

- Mercury Intrusion Porosimetry (MIP) test was performed by means of a Micromeritics AutoPore IV 9500 series mercury intrusion porosimeter.

- Thermal Gravimetric Analysis (TGA) was carried out to study the thermal reduction properties of the samples by means of an SDT Q600 V20.9 Build 20 thermal gravimetric analyser under nitrogen flow at 100 ml/min. Temperature was elevated at a constant heating rate of 10 °C/min between 35 and 1450 °C. Temperature was held constant at 105 °C for 2 h to promote elimination of free water.
- Scanning Electron Microscope (SEM) observations were performed by means of a ZEISS scanning electron microscope equipped with an energy dispersive analyser with a 15 kV accelerating voltage.

Moreover, during the re-cracking stages performed for half of the healing specimens, the load and CMOD data were acquired and related curves, referring to each single pre-cracking/re-cracking event, plotted in series, were also compared to the monotonic flexural toughness curves obtained by testing the specimens in 3-point bending at different ages listed above. Though the exact correspondence may be questioned because of not exactly matching testing ages, the comparison can always provide an insight into the evolution of the mechanical properties of the material, as due to concurrent aging and healing in the intended scenarios.

4. Experimental results

4.1. Compressive and flexural strength and pore structure

The results of compressive strength tests along time can be observed in Fig. 5, together with related experimental scattering as from the six nominally identical tests performed per each mix and at each testing age. As a general trend it can be first of all observed that all the composites were able, irrespective of the curing, to develop an average compressive strength in the 120–160 MPa range at 28 days, complying with their high performance denomination with a coefficient of variation (CoV) ranging from 3 to 10% for each mix. Slight improvements were observed for curing times longer than 28 days; the limitedness of the measured long term strength increase can be explained both considering the rapid hardening cement type employed as well as the low water-binder

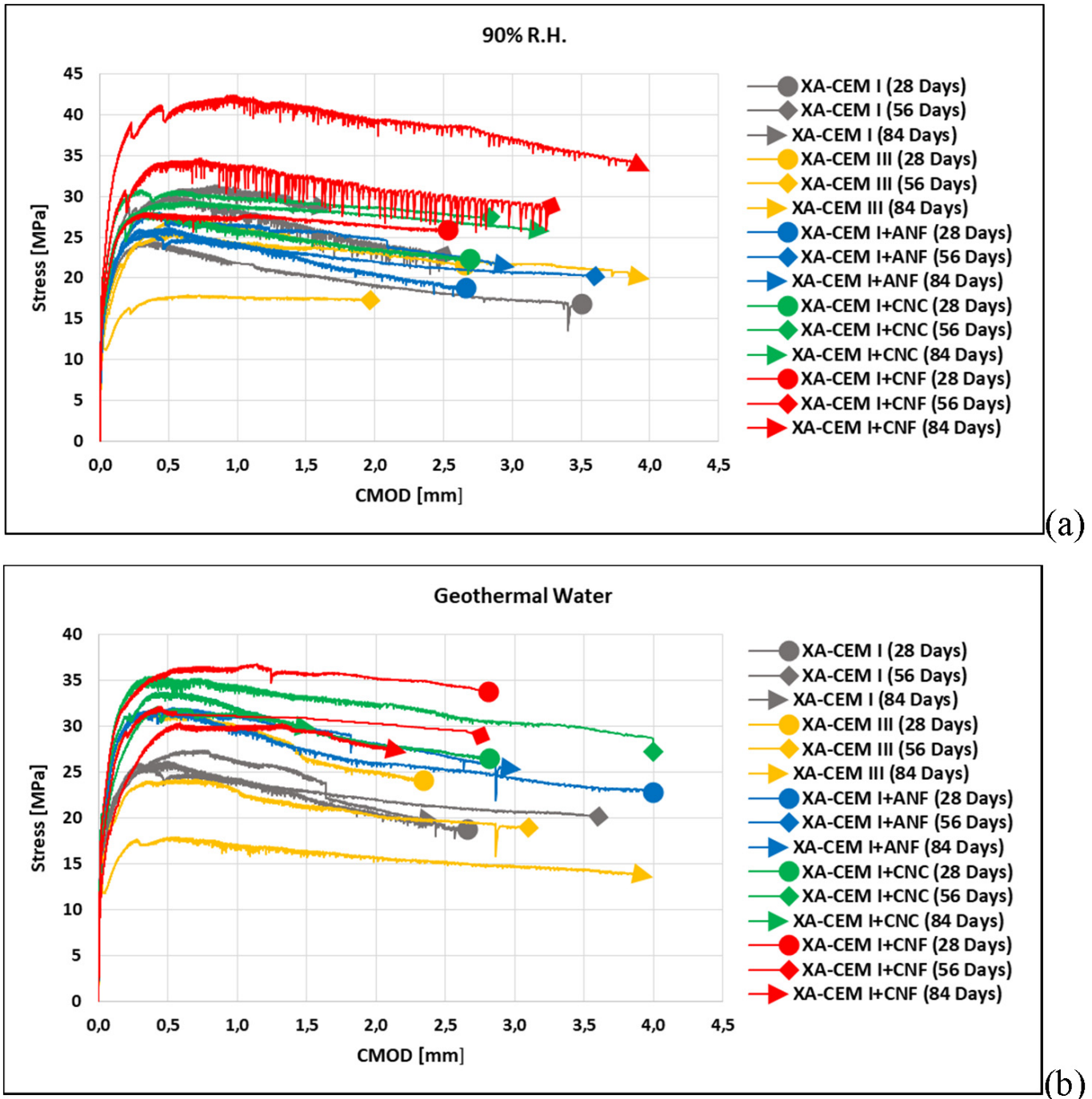


Fig. 9. Average nominal flexural stress vs. CMOD curves for investigated cementitious composites cured in 20 °C-90%RH climate room (a) and in geothermal water (b).

ratio which, limiting from a certain point onward the hydration of cement, is also likely to hinder the long-term hydraulic activity of the slag, which requires calcium hydroxide produced by cement hydration as an activator. Interestingly, curing under water, though containing aggressive species, resulted into somewhat higher strength, likely for the larger availability of the water itself. Effects of nanoparticles are also evident in promoting moderately higher strength, likely due to the aforementioned effects of nuclei of cement hydration, these effects slightly vanishing for longer curing times. It is likely that the water retaining capacity and hydrophilic features of the employed nano-constituents by promoting faster hydration can shadow in the long term the effects of larger water availability.

Fig. 6 shows the flexural strength values along time for which CoV ranged from 6 to 19% for each mix. Moreover, similar statements than for compressive strength hold for flexural strength, in which case it has to be by the way remarked that the improvement provided by nano-constituents is systematically higher when curing under geothermal water and remains basically unchanged along the curing time, whereas the improvements on compressive strength tended to vanish along curing time (Fig. 6). This difference can be explained considering that the improvement in compressive strength can be primarily attributed to matrix densification and pore structure refinement. MIP tests performed on specimens after three month exposure to both the investigated curing conditions confirmed some slight refinement of the pore structure due to

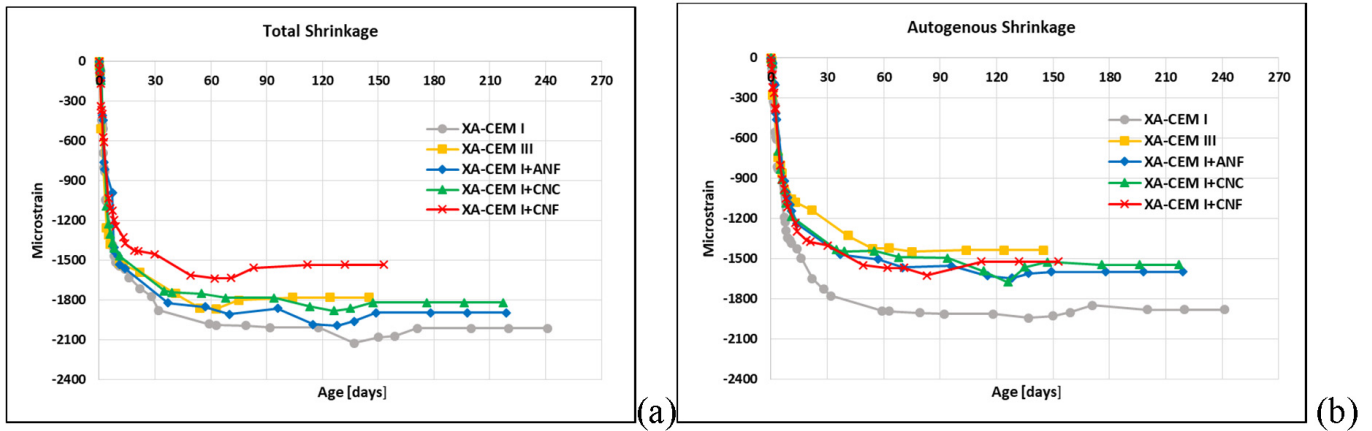
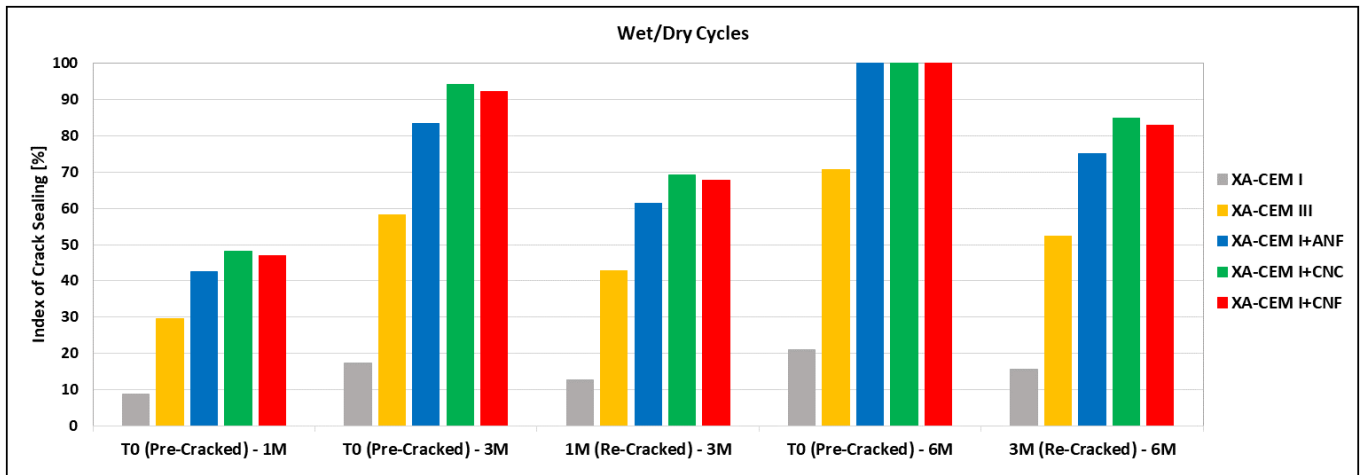
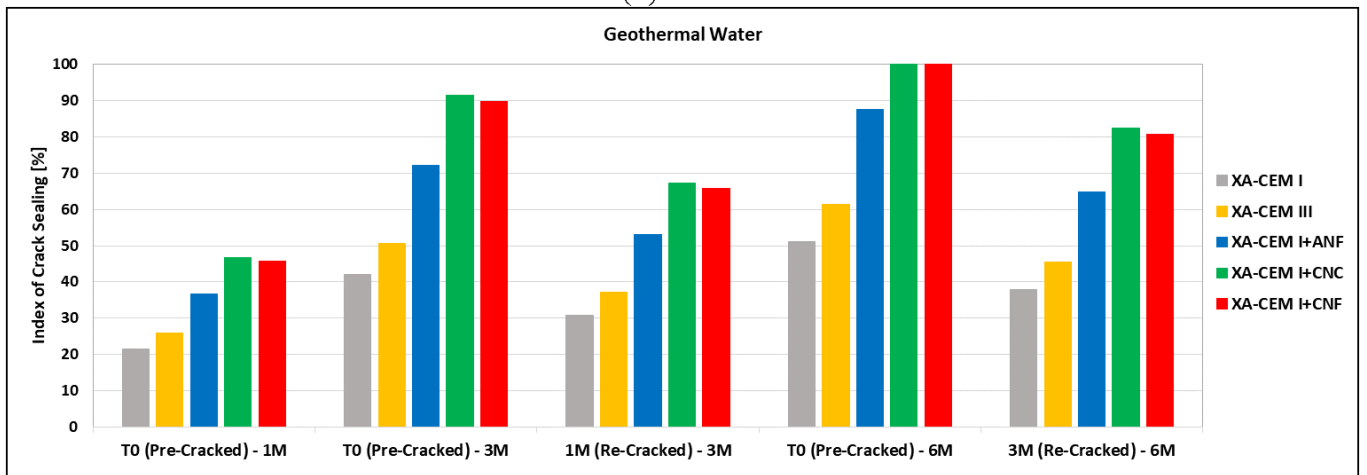


Fig. 10. Total and autogenous shrinkage for investigated cementitious composites.



(a)

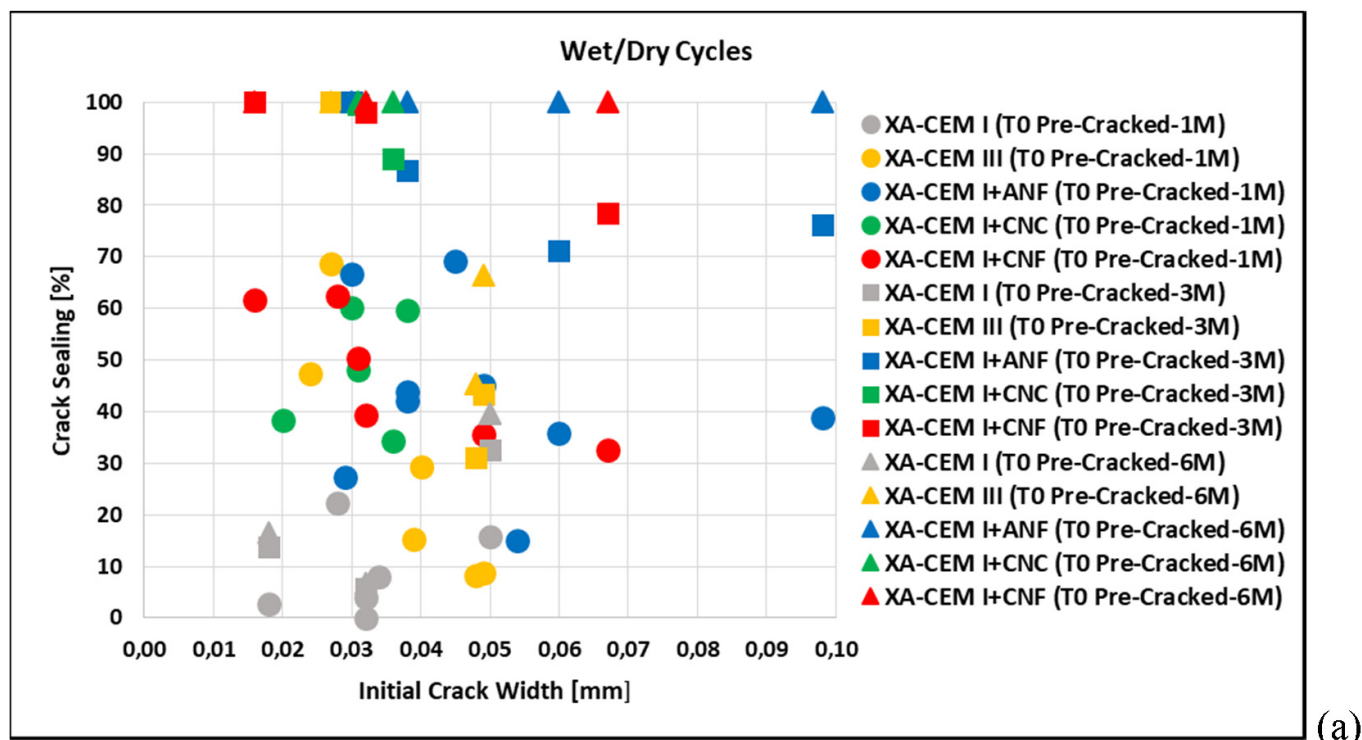


(b)

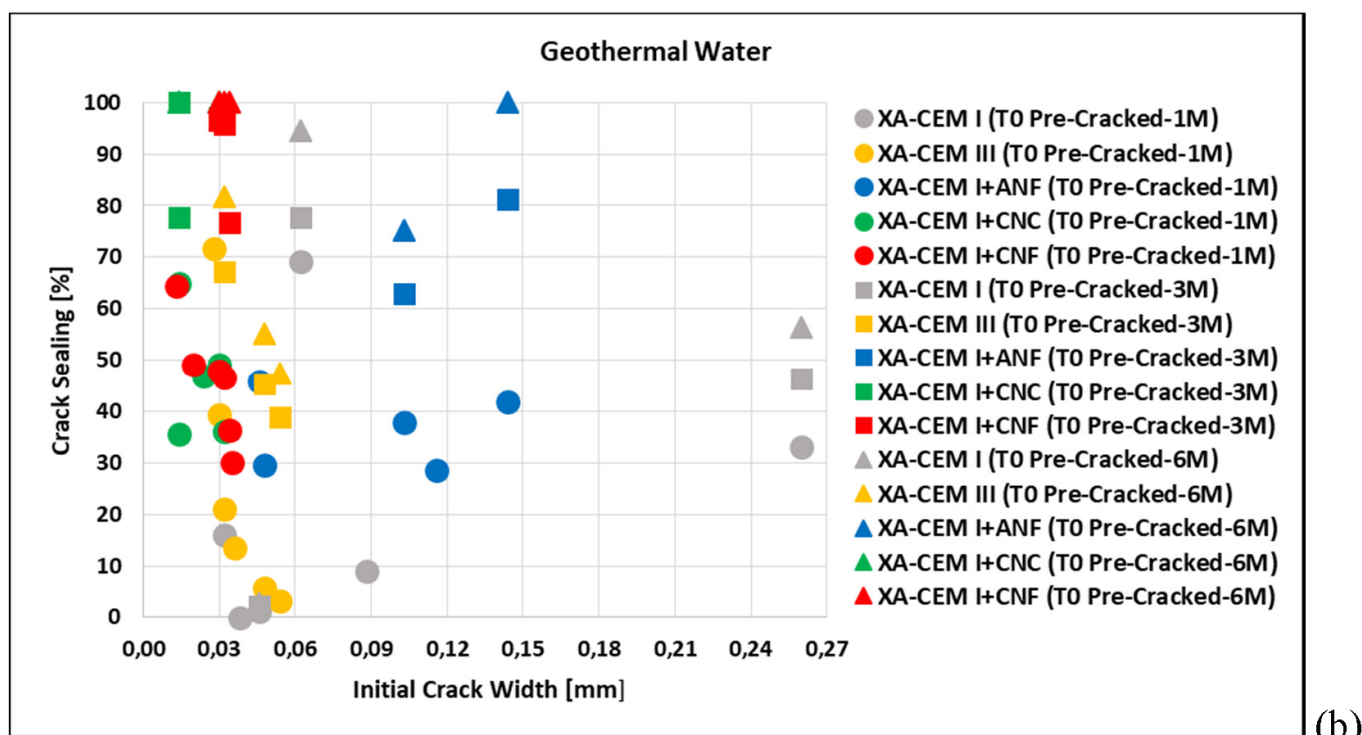
Fig. 11. Index of Crack Sealing (ICS) for investigated cementitious composites cured in wet/dry cycles (a) and in geothermal water (b).

the presence of nano-constituents (Fig. 7). Hence, this pore refinement structure, may, as detected, asymptotically converge to a common bound, evenly smoothing any further improvement in compressive strength.

On the other hand, in flexural behaviour, this same matrix densification effects, which can be also held as responsible of improvements of the fibre–matrix interface, can be hypothesized as acting in synergy with a nano- and micro-scale reinforcement



(a)



(b)

Fig. 12. Crack sealing and initial crack width for investigated cementitious composites cured in wet/dry cycles (a) and in geothermal water (b).

effect provided by the nano-constituents. This improvement is primarily evident in the case of cellulose nano-fibrils, which feature the highest length and aspect ratio among all the nano-constituents employed in the present investigation and hence are likely to better profit and exploit of an improvement at the fibre-matrix interface level.

This assumption is likely to be supported also by SEM images, where the nano-filaments of both cellulose and alumina are

clearly seen as reinforcing the crystalline structure of the hydrated composites (Fig. 8). It is furthermore worth remarking, to provide further support to the hypotheses above, that the same aforesaid trends of flexural strength also hold with reference to the whole flexural behaviour, as from the average nominal flexural stress vs. CMOD curves shown in Fig. 9, which also testify the deflection hardening behaviour of all the investigated composites.

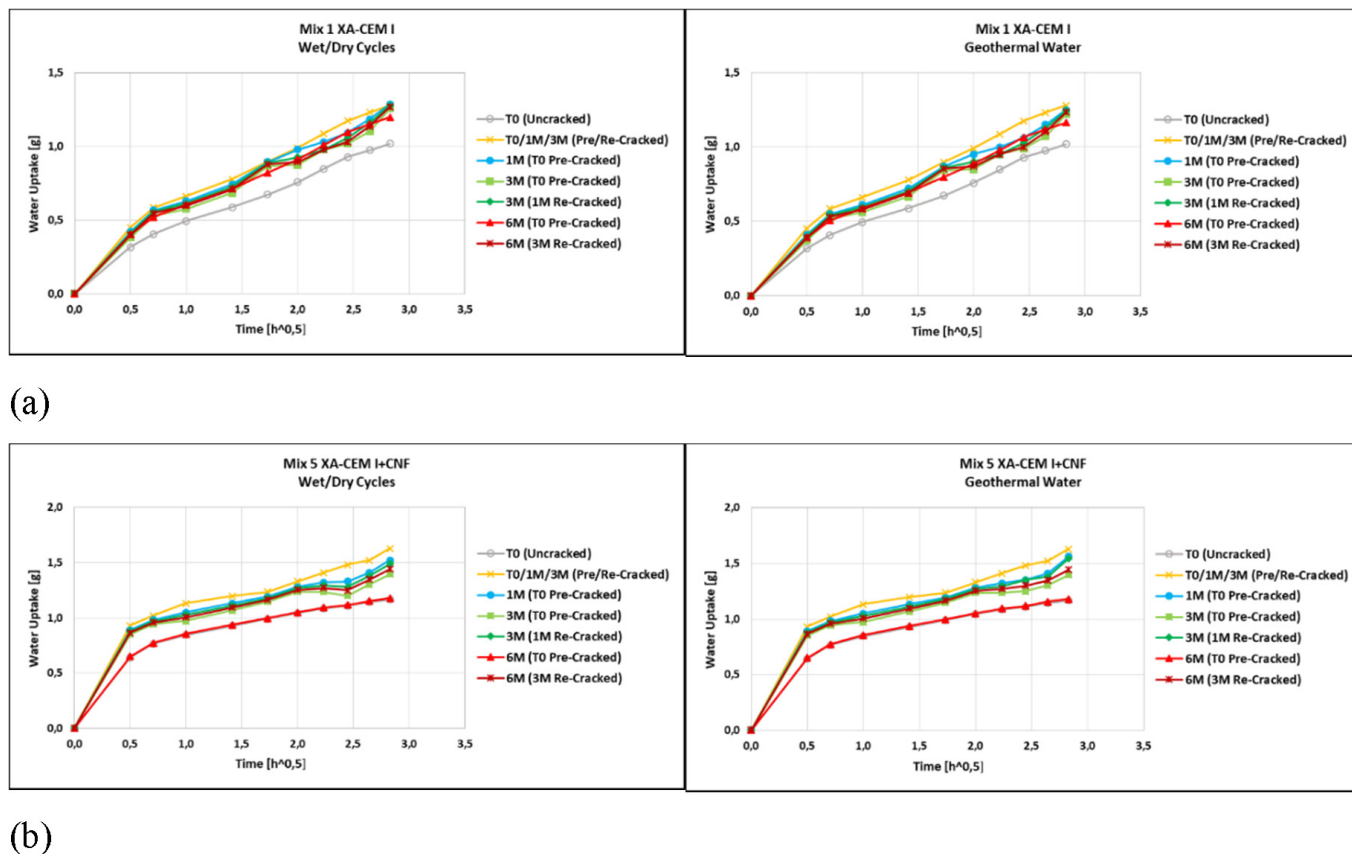


Fig. 13. Typical water uptake vs. square root of time curves for the reference mix (a) and for the mix containing nano-cellulose fibrils (b), for the different healing scenarios and deadlines.

4.2. Autogenous and drying shrinkage

Effects of nanoparticles on matrix densification and pore structure refinement, thanks to aforementioned promotion of material hydration, are also confirmed by the measured development, up to eight months, of total drying and autogenous shrinkage (Fig. 10). Fig. 10 shows the average curves for each 3 identical mixes. For autogenous shrinkage test results at 100 days, the CoV for each mix was up to 1.05% for XA-CEM I, 4.39% for XA-CEM III, 1.99% for XA-CEM I + ANF, 3.54% for XA-CEM I + CNC and 1.02% for XA-CEM I + CNF.

For drying (total) shrinkage test results at 100 days, the CoV for each mix was up to 4.92% for XA-CEM I, 1.83% for XA-CEM III, 4.83% for XA-CEM I + ANF, 2.41% for XA-CEM I + CNC and 4.55% for XA-CEM I + CNF.

All the investigated nano-constituents have similar (about 20%) reduction effect on autogenous shrinkage development which, as a matter of fact, accounts for up to more than 80% of the total shrinkage deformation. Different efficacy on the total drying shrinkage have been measured, cellulose nano-fibrils providing the most significant reduction also in this case.

The results are coherent with previous literature findings about the efficacy of nano-cellulose products in acting as effective internal curing promoters in HPRCCs [40].

4.3. Crack sealing

Visual inspection of the cracks and image analysis of the evolution of their total area and width along the healing period (see Fig. 4) constitutes the first step in the assessment of crack self-sealing and material self-healing capacity [50]. It is well-known

that self-sealing and self-healing results have a strong dependency with the crack width and the internal crack geometry [51].

Effects of the employed nano-constituents on the crack-sealing capacity (Index of Crack Sealing calculated as explained in Section 3) clearly appear since the earlier curing times and continues to develop along it up to the investigated six-month deadline. Significantly, it can be observed that in the presence of nano-constituent, the same crack sealing capacity was measured for both immersed specimens as well as for samples subjected to wet-and-dry cycles (Fig. 11). Moreover, considering the experimental scattering, the crack-sealing performance turned out to be scantily sensitive to the initial crack opening, which anyway in all the investigated mixes, remained below 0.1 mm in almost all the cases, and in most of them in the range of few tens of microns (Fig. 12).

Experimental results also demonstrated the repeatability of the crack-sealing capacity in the case of re-cracking after one and three months healing deadlines and significantly, both in the case of the crystalline admixture alone, for which this specific feature was already highlighted by [46,47] and in the case of synergy action with each and all of the investigated nano-constituents.

As a matter of fact, specimens which underwent an intermediate re-cracking after one month, retained 70–80% of their crack sealing capacity at the three-month deadline, as compared to specimens continue to healing undisturbedly immersed for three months, and a somewhat lower 60–70% of this capacity if healing occurred under wet-and-dry cycles. The same healing capacity continued to be retained by the same specimens after having undergone a further re-cracking after three months healing and when checked at six-month deadline, as compared to specimens undergoing continuous healing undisturbed for six months.

4.4. Sorptivity tests and healing-induced recovery of durability performance

Fig. 13 show typical water uptake vs. square root of time curves for the reference mix specimens and for samples made with the mix containing nano-cellulose fibrils, for the different healing scenarios and deadlines. Similar trends also hold for all other investigated cementitious composites reinforced with the different employed nano-constituents.

The effects of crack-sealing on the progressive recovery of water-tightness vs capillary absorption are clearly evident and have been furthermore confirmed by the elaboration of data referring to the calculation of the sorptivity coefficient and related Index of Sorptivity Healing, as defined in Section 3. Data shown in Fig. 14 confirm the same trends already highlighted before with reference to the Index of Crack Sealing, i.e.:

- Nano-constituents, in synergy with the crystalline admixture, promote a more effective and faster healing already after one month and almost irrespective of the healing scenario, though they seem to perform slightly better under wet-and-dry cycles. Though added at a very low dosage, it can be likely guessed that their activity is favoured when the water absorbed during the wet period is allowed to be released and distributed throughout the bulk material during the drying stage, thus also renovating their capacity.
- The repeatability and persistence of the healing capacity after repeated cycles of cracking and healing is confirmed also with reference to the water-tightness vs capillary water absorption.

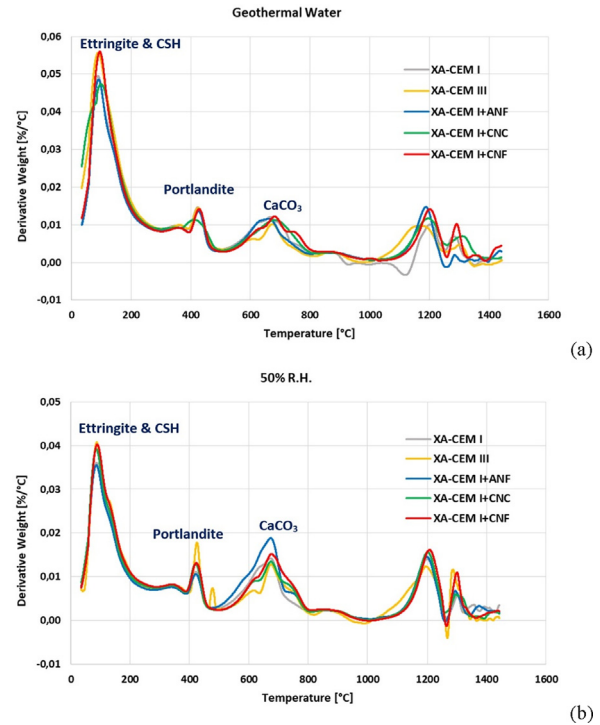


Fig. 15. DTGA curves of samples extracted in the vicinity of cracks healed in different regimes: a) geothermal water and b) 50%R.H.

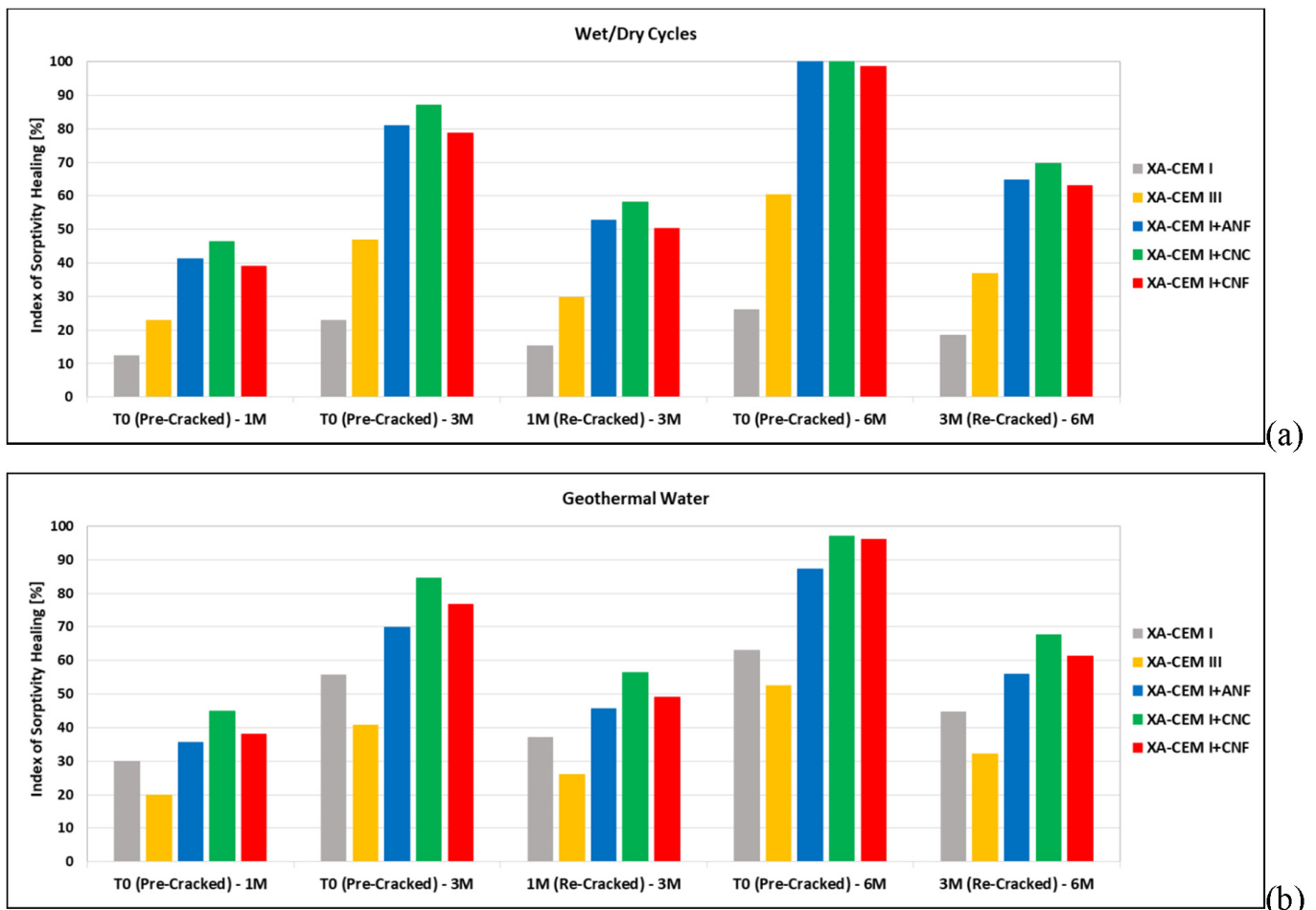
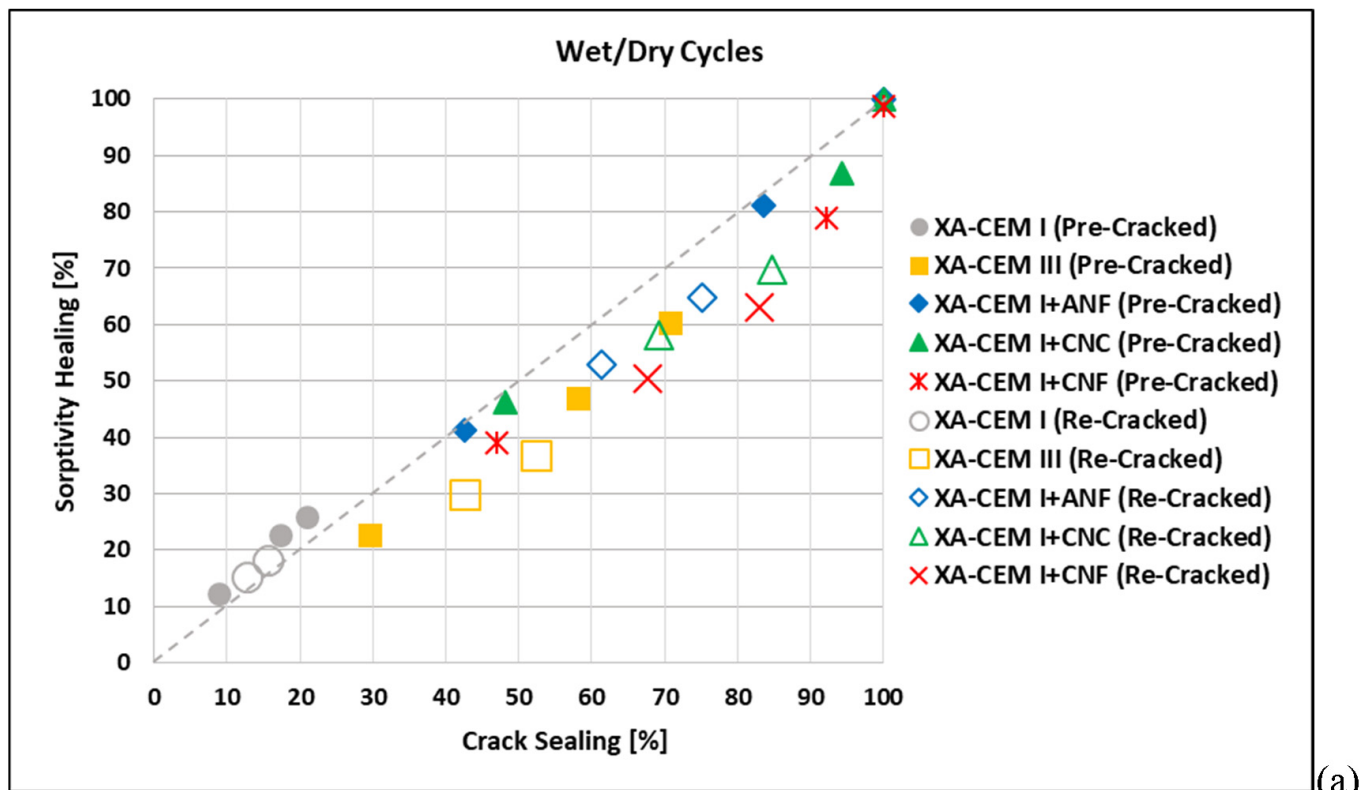
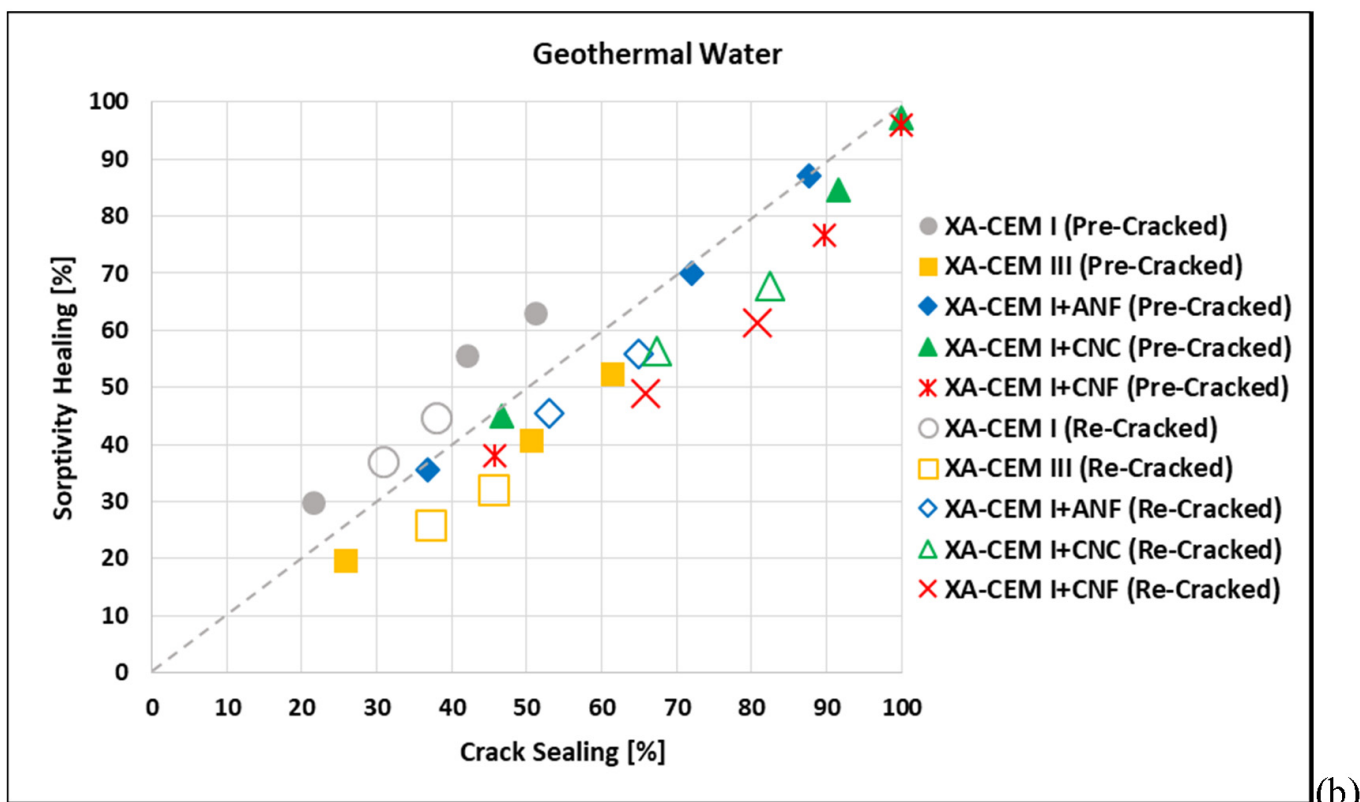


Fig. 14. Index of Sorptivity Healing (ISH) for investigated cementitious composites cured in wet/dry cycles (a) and in geothermal water (b).



(a)



(b)

Fig. 16. Index of material durability-performance healing vs. Index of Crack Sealing.

In this case the predominant effect seems to be due to the crystalline admixture which, e.g., in the case of specimens repeatedly cracking after one month and three months healing is able to guarantee, at the six-months cumulative deadline, more than 70% of the healing capacity of companion specimens

undergoing an as much as long continuous undisturbed healing, both under continuous immersion and exposure to wet-and-dry cycles. Such a retaining capacity is slightly lower with the further presence of nano-additions, in the 60–70% range, and always somewhat better under the wet-and-dry cycle

exposure, confirming the aforesaid assumption. The hydrophilic properties of the nano-constituents can be claimed to justify this data.

The beneficial effects of the nano-constituents appear to be connected to the nano- and micro-structure reinforcement effect as well as to their internal curing effectiveness. This is further confirmed by the TGA/DTGA analyses of samples extracted in the vicinity of the healed cracks, which showed, for all the investigated mixes, absolutely similar trends, highlighting delayed hydration (CSH peak) and carbonation (CaCO₃ peak) as the main reactions responsible of healing (Fig. 15).

4.5. Material performance healing vs. crack sealing

The coherence of the whole garnered and analysed set of data is further confirmed by the plots of the material durability performance healing index as a function of the crack sealing effectiveness, which appear to be strongly correlated to each other (Fig. 16).

Though all data fall in a very narrow experimental scattering, it is interesting to observe that data of the reference mix are likely to show a durability performance healing index higher than the crack sealing index proportionality, the opposite occurring for all the mix with nano-constituents. This can be once again explained considering the hydrophilic features of the employed nano-particles, which, though through a healed and healing crack, continuous to be active fostering some higher absorption of water.

5. Concluding remarks

In this study the healing capacity in aggressive scenarios (geothermal water) has been studied of High Performance Fibre Reinforced Cementitious Composites, as stimulated by crystalline admixtures and further enhanced by the synergy action of either alumina nanofibers or nano-cellulose fibrils and crystals. The persistence and repeatability of such a capacity has been also checked in front of cycles of cracking and healing both under permanent immersion or exposure to wet and dry cycles in geothermal water obtained from cooling tower basins in a geothermal power plant operated by Enel Green Power in Tuscany. The healing performance has been assessed by both visual crack inspection and recovery of the water-tightness vs. water capillary absorption with the purpose of validating an innovative concept of Ultra High Durability Concrete to be employed into novel design and construction concept of water basins and mud tanks servicing the same geothermal plants.

From the experimental results presented and discussed in this paper the following conclusions hold:

- Employed nano-constituents are able to induce and improvement of the mechanical performance of the investigated Ultra High Performance Cementitious Composites, especially when cured, since immediately after casting, under the aforesaid aggressive scenario. This effect is due to a synergy between pore refinement and matrix densification functionalities, further confirmed by reduction in autogenous shrinkage, which remarks the internal curing capacity of the employed nano-additions, with a reinforcement effect provided at the very crystalline structure level, already highlighted by some literature studies and further confirmed by SEM imaging in the present work.
- Thanks to the same aforementioned effects, nano-constituents enhance and accelerate the autogenous healing capacity of the investigated cementitious composites, as stimulated by the

employed crystalline admixture. The hydrophilic action of the nano-constituents appears to be better effective under wet and dry cycles exposure, since, reasonably, the absorbed water needs to be released throughout the bulk material and at the healed cracked sites in order to continue being effective. On the other hand, continuous immersion may rapidly saturate the aforementioned capacity.

- The crystalline admixture provides its most significant effect in guaranteeing the highest persistence and repeatability of the healing capacity after repeated cracking and healing cycles. At six months healing schedule, it guarantees the permanence of 70% of the healing capacity in specimens undergoing two re-cracking after one and three months as compared to specimens experiencing continuous six months healing.
- Correlation of performance healing (recovery of water-tightness vs. capillary water absorption) vs. crack sealing efficiency confirmed the robustness and consistency of the whole set of data produced and discussed in the present investigation. Interestingly, while for the reference mix fell above the $y = x$ correlation line, all data for the mixes with nano-constituents fall below it, likely because of the same hydrophilic features which continued to be active also through the healing and healed cracks.
- TGA/DTGA analyses confirmed for all the investigated cementitious composites delayed hydration and carbonation as the healing mechanisms, the latter prevailing under wet and dry cycles exposure.

This study hence provides a solid database for the validation of the Ultra High Durability Concrete concept the H2020 project ReSHEALience consortium is currently working on. This aims to produce a breakthrough paradigm shift in the durability-based conceptual design of cement based construction materials, from mere providers of passive protection against the ingress of aggressive species in the structure to active players able to govern the evolution of their performance under the intended aggressive structural service scenarios.

CRediT authorship contribution statement

Estefania Cuenca: Conceptualization, Methodology, Formal analysis, Validation, Investigation, Data curation, Writing - original draft, Writing - review & editing. **Alessandro Mezzena:** Methodology, Investigation, Data curation. **Liberato Ferrara:** Conceptualization, Methodology, Formal analysis, Validation, Writing - original draft, Writing - review & editing, Supervision, Funding acquisition.

Declaration of Competing Interest

The authors declare that they have no known competing financial interests or personal relationships that could have appeared to influence the work reported in this paper.

Acknowledgements

The research activity reported in this paper has been performed in the framework of the **ReSHEALience project (Rethinking coastal defence and Green-energy Service infrastructures through enHancEd-durAbiLiTy high-performance cement-based materials)** which has received funding from the European Union's Horizon 2020 research and innovation program under grant agreement No 760824. The information and views set out in this publication do not necessarily reflect the official opinion of the European Commission.

The kind collaboration of ReSHEALience partners ANF Development (dr. Alexej Tretjakov and dr. Dennis Lizunov), API-Europe

(Mrs. Stamatina Sideri and Dr. Evangelia Nteze) and Penetron Italia (Mr. Enrico Maria Gastaldo Brac) in supplying respectively alumina nano-fibres, cellulose nano-fibrils and crystals and the crystalline self-healing promoter is also acknowledged. Kind help of Mr. Francesco Animato, Mrs. Sandra Scalari and Mr. Iacopo Mazzantini in allowing visits to Enel Green Power geothermal plants in Tuscany for geothermal water supply is also acknowledged.

The authors also thank Mr. Marco Francini (Buzzi Unicem) for supplying of cement, Mr. Michele Gadioli and Roberto Rosignoli (Azichem Ltd) for supplying of steel fibres and Mr. Sandro Moro (BASF Italia) for supplying the superplasticizer employed for casting the different investigated UHDC mixes. The cooperation is acknowledged of MEng. Waqar Ahmed and MEng. Muhammad Awais in performing the first phase of the mechanical and self-healing tests, in partial fulfilment of the requirements for the MEng. in Civil Engineering. Last but not least the help of Mr. Antonio Cocco and Mr. Paolo Broglio, Laboratory for Testing Materials, Buildings and Structures, Politecnico di Milano in casting specimens for the experimental programme and providing organizational support for its execution is gratefully acknowledged.

References

- [1] A.E. Naaman, H.W. Reinhardt, Proposed classification of HPFRCC composites based on their tensile response, *Mater. Struct.* 39 (5) (2006) 547–555.
- [2] G.J. Parra-Montesinos, H.W. Reinhardt, High Performance Fiber Reinforced Cement Composites 6', eds. Naaman, A., RILEM Bookseries, Springer, 2012.
- [3] V.H. Perry, What really is ultra-high performance concrete? – Towards a global definition, in: C. Shi, B. Chen, (Eds.), Proceedings of the 2nd International Conference on UHPC materials and structures, UHPC 2018-China, Fuzhou, China, 7–10 November 2018, RILEM Pubs. S.A.R.L., pp. 89–105.
- [4] NF P 18-710: National addition to Eurocode 2 – Design of concrete structures: specific rules for Ultra-High Performance Fibre-Reinforced Concrete (UHPRFC) – April, 2016.
- [5] E. Cuenca, L. Ferrara, Self-healing capability of Fiber Reinforced Concretes. State of the art and perspectives, *J. Korean Soc. Civil Eng.* 21 (7) (2017) 2777–2789.
- [6] L. Ferrara, V. Krelani, F. Moretti, M. Roig Flores, P. Serna Ros, Effects of autogenous healing on the recovery of mechanical performance of High Performance Fibre Reinforced Cementitious Composites (HPFRCCs): part 1, *Cem. Concr. Compos.* 83 (2017) 76–100.
- [7] L. Ferrara, V. Krelani, F. Moretti, Autogenous healing on the recovery of mechanical performance of High Performance Fibre Reinforced Cementitious Composites (HPFRCCs): part 2 – correlation between healing of mechanical performance and crack sealing, *Cem. Concr. Compos.* 73 (2016) 299–315.
- [8] D. Homma, H. Mihashi, T. Nishiwaki, Self-healing capability of fibre reinforced cementitious composites, *J. Adv. Concr. Technol.* 7 (2) (2009) 217–228.
- [9] D. Kim, S. Kang, T. Ahn, Mechanical characterization of high-performance steel-fiber reinforced cement composites with self-healing effect, *Materials* 7 (1) (2014) 508–526.
- [10] M. Şahmaran, G. Yildirim, T.K. Erdem, Self-healing capability of cementitious composites incorporating different supplementary cementitious materials, *Cem. Concr. Compos.* 35 (2013) 89–101.
- [11] E. Özbay, M. Şahmaran, H. Yücel, T. Erdem, M. Lachemi, V. Li, Effect of sustained flexural loading on Self-Healing of Engineered Cementitious Composites, *J. Adv. Concr. Technol.* 11 (2013) 167–179.
- [12] M. Şahmaran, S.B. Keskin, G. Ozerkan, et al., Self-healing of mechanically-loaded self-consolidating concretes with high volumes of fly ash, *Cem. Concr. Compos.* 30 (10) (2008) 872–879.
- [13] M. Şahmaran, V. Li, Durability of mechanically loaded engineered cementitious composites under highly alkaline environments, *Cem. Concr. Compos.* 30 (2008) 72–81.
- [14] M. Şahmaran, G. Yildirim, R. Noori, E. Özbay, M. Lachemi, Repeatability and pervasiveness of self-healing in engineered cementitious composites, *ACI Mater. J.* 112 (4) (2015) 513–522.
- [15] V. Li, Y. Lim, Y. Chan, Feasibility of a passive smart self-healing cementitious composite, *Compos. B Eng.* 29 (1998) 819–827.
- [16] M. Li, V. Li, Cracking and healing of engineered cementitious composites under chloride environment, *ACI Mater. J.* 108 (3) (2011) 333–340.
- [17] T. Nishiwaki, S. Kwon, D. Homma, M. Yamada, H. Mihashi, Self-healing capability of Fiber-Reinforced Cementitious Composites for recovery of watertightness and mechanical properties, *Materials* 7 (2014) 2141–2154.
- [18] L. Ferrara, S.R. Ferreira, V. Krelani, P. Lima, F.de A. Silva, R.D. Toledo Filho, Cementitious composites reinforced with natural fibers, in: J.A.O. Barros, et al., (Eds.) Recent advances on green concrete for structural purposes. The contribution of the EU-FP7 project EnCoRe, Springer, pp. 427+x, ISBN 978-3-319-56797-6 (2017).
- [19] D. Snoeck, N. De Belie, Mechanical and self-healing properties of cementitious composites reinforced with flax and cottonised flax, and compared with polyvinyl alcohol fibres, *Biosyst. Eng.* 111 (2012) 325–334.
- [20] D. Snoeck, K. Van Tittelboom, S. Steuoperaert, P. Dubrueel, N. De Belie, Self-healing cementitious materials by the combination of microfibers and superabsorbent polymers, *J. Intell. Mater. Syst. Struct.* 25 (1) (2014) 13–24.
- [21] D. Snoeck, N. De Belie, From straw in bricks to modern use of microfibers in cementitious composites for improved autogenous healing. A review, *Constr. Build. Mater.* 95 (2015) 774–787.
- [22] D. Snoeck, P. Smetryns, N. De Belie, Improved multiple cracking and autogenous healing in cementitious materials by means of chemically-treated natural fibres, *Biosyst. Eng.* 139 (2015) 87–99.
- [23] D. Snoeck, N. De Belie, Repeated autogenous healing in strain-hardening cementitious composites by using superabsorbent polymers, *ASCE J. Mater. Civil Eng.* 28 (1) (2016) 1–11.
- [24] D. Snoeck, J. Dewanckele, V. Cnudde, N. De Belie, X-ray computed microtomography to study autogenous healing of cementitious materials promoted by superabsorbent polymers, *Cem. Concr. Compos.* 65 (2016) 83–93.
- [25] L. Ferrara, V. Krelani, F. Moretti, On the use of crystalline admixtures in cement based construction materials: from porosity reducers to promoters of self healing, *Smart Mater. Struct.*, 25 (2016) 084002 (17pp).
- [26] P. Escoffres, C. Desmettre, J.P. Charron, Effect of a crystalline admixture on the self-healing capability of high-performance fiber reinforced concretes in service conditions, *Constr. Build. Mater.* 173 (2018) 763–774.
- [27] E. Cuenca, S. Rigamonti, E. Gastaldo-Brac, L. Ferrara, Crystalline admixture as healing promoter in concrete exposed to chloride-rich environments: an experimental study, *J. Mater. Civil Eng.* DOI: 10.1061/(ASCE)MT.1943-5533.0003604.
- [28] L. Ferrara, P. Bamonte, C.S. Falcó, F. Animato, C. Pascale, A. Tretjakov, E.T. Camacho, P. Deegan, S. Sideri, E.M. Gastaldo Brac, P. Serna, V. Mechtcherine, M. C. Alonso, A. Peled, R.P. Borg, An overview on H2020 project “Reshealience”, in: Proceeding IABSE Symposium, Guimaraes 2019: Towards a Resilient Built Environment Risk and Asset Management (2019), pp. 184–191.
- [29] S. Muzenski, I. Flores-Vivian, K. Sobolev, Ultra-high strength cement-based composites designed with aluminum oxide nano-fibers, *Constr. Build. Mater.* 220 (2019) 177–186.
- [30] S. Muzenski, I. Flores-Vivian, K. Sobolev, Hydrophobic modification of ultra-high-performance fiber-reinforced composites with matrices enhanced by aluminum oxide nano-fibers, *Constr. Build. Mater.* 244 (2020) 118354.
- [31] P. McElroy, H. Emadi, D. Unruh, Permeability and elastic properties assessment of alumina nanofiber (ANF) cementitious composites under simulated wellbore cyclic pressure, *Constr. Build. Mater.* 239 (2020) 117867.
- [32] P. Jaishankar, C. Karthikeyan, Characteristics of Cement Concrete with Nano Alumina Particles, in: IOP Conference Series: Earth and Environmental Science, 80(1) (2017), paper 012005, IOP Publishing.
- [33] K. Behfarnia, N. Salemi, The effects of nano-silica and nano-alumina on frost resistance of normal concrete, *Constr. Build. Mater.* 48 (2013) 580–584.
- [34] R. Gowda, H. Narendra, D. Rangappa, R. Prabhakar, Effect of nano-alumina on workability, compressive strength and residual strength at an elevated temperature of Cement Mortar, *Mater. Today: Proc.* 4 (11) (2017) 12152–12156.
- [35] T. Fu, R. Moon, P. Zavaterra, J. Youngblood, J. Weiss, Cellulose nanomaterials as additives for cementitious materials' in: Cellulose-Reinforced Nanofibre Composites, eds. Jawaid, M., Boufi, S., Khalil, A. (2017), 455–482.
- [36] M. Ardanyu, J. Claramunt, R. Arevalo, F. Pares, E. Aracri, T. Vidal, Nanofibrillated cellulose (NFC) as a potential reinforcement for high-performance cement mortar composites, *Bioresources* 7 (3) (2012) 3883–3894.
- [37] R. Mejdoub, H. Hammi, J.J. Sunol, M. Khitouni, A. M'nif, S. Boufi, Nanofibrillated cellulose as nano reinforcement in Portland cement: thermal, mechanical and microstructural properties, *J. Compos. Mater.* 0(0) (2016) 1–13.
- [38] Y. Cao, P. Zavaterra, J. Youngblood, R. Moon, J. Weiss, The influence of cellulose nanocrystal additions on the performance of cement paste, *Cem. Concr. Compos.* 56 (2015) 73–83.
- [39] Y. Cao, P. Zavaterra, J. Youngblood, R. Moon, J. Weiss, The relationship between cellulose nanocrystal dispersion and strength, *Constr. Build. Mater.* 119 (2016) 71–79.
- [40] L. Ferrara, S.R. Ferreira, M. Della Torre, V. Krelani, F. Silva, R.D. Toledo Filho, Effect of cellulose nanopulp on autogenous and drying shrinkage of cement based composites, in *Nanotechnology in Construction*, Proceedings Nicom 5, K. Sobolev and S.P. Shah, eds., Springer, Chicago, 26–28 May 2015, pp. 325–330, ISBN 9783319170879.
- [41] L. Ferrara, N. Ozyurt, M. di Prisco, High mechanical performance of fiber reinforced cementitious composites: the role of “casting-flow” induced fiber orientation, *Mater. Struct.* 44 (1) (2011) 109–128.
- [42] M. di Prisco, L. Ferrara, M.G.L. Lamperti, Double Edge Wedge Splitting (DEWS): an indirect tension test to identify post-cracking behaviour of fibre reinforced cementitious composites, *Mater. Struct.* 46 (11) (2013) 1893–1918.
- [43] L. Ferrara, V. Krelani, M. Carsana, A fracture testing based approach to assess crack healing of concrete with and without crystalline admixtures, *Constr. Build. Mater.* 68 (2014) 515–531.
- [44] M. Roig-Flores, S. Moscato, P. Serna, L. Ferrara, Self-healing capability of concrete with crystalline admixtures in different environments, *Constr. Build. Mater.* 86 (2015) 1–11.
- [45] M. Roig Flores, F. Pirritano, P. Serna Ros, L. Ferrara, Effect of crystalline admixtures on the self-healing capability of early-age concrete studied by

- means of permeability and crack closing tests, *Constr. Build. Mater.* 114 (2016) 447–457.
- [46] E. Cuenca, A. Tejedor, L. Ferrara, A methodology to assess crack sealing effectiveness of crystalline admixtures under repeated cracking-healing cycles, *Constr. Build. Mater.* 179 (2018) 619–632.
- [47] E. Cuenca, L. Ferrara, Fracture toughness parameters to assess crack healing capacity of fiber reinforced concrete under repeated cracking-healing cycles, *Theor. Appl. Fract. Mech.* 106 (102468) (2020) 1–12.
- [48] E. Cuenca, E. Nteze, M. Iakovlev, S. Sideri, L. Ferrara, Microstructural investigation into the effects of nano-cellulose in improving the performance of cementitious materials in acid environments, submitted to *Microdurability 2020*, The 4th International RILEM conference Microstructure Related Durability of Cementitious Composites, Den Haag, The Netherlands, 12-14 October 2020.
- [49] P. Bamonte, S. Al Obaidi, F. Animato, F. Lo Monte, I. Mazzantini, S. Scalari, L. Ferrara, Innovative design concept of cooling water tanks/basins in geothermal power plants using ultra high performance fibre reinforced concrete with enhanced durability, in: *Proceedings of BEFIB2020 - RILEM-fib X International Symposium on Fibre Reinforced Concrete*, 21-23 September 2020, Valencia, Spain.
- [50] L. Ferrara, T. Van Mullem, M.C. Alonso, P. Antonaci, R.P. Borg, E. Cuenca, A. Jefferson, P.L. Ng, A. Peled, M. Roig, M. Sanchez, C. Schroefl, P. Serna, D. Snoeck, J.M. Tulliani, N. De Belie, Experimental characterization of the self-healing capacity of cement based materials and its effects on the material performance: a state of the art report by COST Action SARCOS WG2, *Constr. Build. Mater.* 167 (2018) 115–142.
- [51] T. Van Mullem, E. Gruyaert, B. Debbaut, R. Caspeele, N. De Belie, Novel active crack width control technique to reduce the variation on water permeability results for self-healing concrete, *Constr. Build. Mater.* 203 (2019) 541–551.